Chinese Chemical Letters 33 (2022) 1308–1312

Contents lists available at ScienceDirect

Chinese Chemical Letters

journal homepage: www.elsevier.com/locate/cclet

Microfluidics embedded with microelectrodes for electrostimulation of neural stem cells proliferation

Qian Li[a,b], Bodong Kang[a,b], Libin Wang[a,b], Tao Chen[a,b,*], Yu Zhao[a,b], Shilun Feng[c,*], Rongjing Li[a,b], Hongtian Zhang[d]

[a] Institute of Advanced Photonics Technology, Faculty of Materials and Manufacturing, Beijing University of Technology, Beijing 100124, China
[b] Key Laboratory of Trans-scale Laser Manufacturing Technology (Beijing University of Technology), Ministry of Education, Beijing 100124, China
[c] State Key Laboratory of Transducer Technology, Shanghai Institute of Microsystem and Information Technology, Chinese Academy of Sciences, Shanghai 200050, China
[d] Department of Neurosurgery, The 7th Medical Center, General Hospital of the Chinese People's Liberation Army, Beijing 100700, China

ARTICLE INFO

Article history:
Received 26 May 2021
Revised 5 July 2021
Accepted 2 August 2021
Available online 8 August 2021

Keywords:
Microfluidics
Microelectrode
Electrical stimulation
NSCs
Proliferation

ABSTRACT

The regeneration of the injured nerve and recovery of its function have brought attention in the medical field. Electrical stimulation (ES) can enhance the cellular biological behavior and has been widely studied in the treatment of neurological diseases. Microfluidic technology can provide a cell culture platform with the well-controlled environment. Here a novel microfluidic/microelectrode composite microdevice was developed by embedding the microelectrodes to the microfluidic platform, in which microfluidics provided a controlled cell culture platform, and ES promoted the NSCs proliferation. We performed ES on rat neural stem cells (NSCs) to observe the effect on their growth, differentiation, proliferation, and preliminary explored the ES influence on cells *in vitro*. The results of immunofluorescence showed that ES had no significant effect on the NSCs specific expression, and the NSCs specific expression reached 98.9% ± 0.4% after three days of ES. In addition, ES significantly promoted cell growth and the cell proliferation rate reached 49.41%. To conclude, the microfluidic/microelectrode composite microdevice can play a positive role in the nerve injury repair and fundamental research of neurological diseases.

With the intensification of population aging, faster pace of life, changes in lifestyle, the incidence of central nervous system (CNS) diseases such as Parkinson, epilepsy, and stroke have increased dramatically. These chronic diseases are difficult to be cured, and they not only bring great inconvenience to patients and their families but also increase the burden of society. Traditional treatment of CNS diseases is mainly carried out through drug regulation and surgery. Studies reported among about 50 million epilepsy patients in the world, about 30% of them cannot be effectively controlled by medication alone [1], and long-term use has big side effects. In addition, surgical treatment has certain risks and challenges, and postoperative sequelae may appear. Therefore, there is an urgent need to find new safe and effective treatments for CNS diseases.

In the last two decades, implantable electrical nerve stimulation therapy has been continuously developed. Researches on the treatment of CNS diseases such as Parkinson's disease and epilepsy through electrical stimulation (ES) has also been more extensive [2–4]. The implantable nerve electrical stimulator was composed of a micro-electric pulse generator and a nerve electrode. The former sent out electric pulses, and the latter applied electric pulses to the target tissue. Nerve electrodes can be divided into rigid and flexible according to the properties of the matrix material. Rigid electrodes are generally made of silicon-based materials, which have good biocompatibility and are easy to be processed, but they are likely to cause large tissue damage after implantation. Flexible electrodes are generally made of flexible polymers, which have good compatibility with organisms. Kim *et al.* [5] reported a cortical electrode composed of ultra-thin plastic layer, silk material, and slender metal electrode. When attached to the surface of the cerebral cortex, it can receive brain wave signals and contribute to the treatment of neurological diseases. When nerve cells are stimulated, electronegative nerve cells can generate a weak localized electric field, which in turn will increase the internal electric field, and help stabilize the bioelectric properties of cell membranes, and promote the growth and regeneration of nerve tissue [6–8]. Zhu *et al.* [9] conducted electrical stimulation of NSCs on carbon nanofiber scaffolds and found that ES could affect NSCs behav-

* Corresponding authors.
E-mail addresses: chentao@bjut.edu.cn (T. Chen), shilun.feng@mail.sim.ac.cn (S. Feng).

https://doi.org/10.1016/j.cclet.2021.08.006
1001-8417/

iors. Xiao *et al.* [10] stimulated PC12 cells and the result showed that ES could affect the differentiation of the cells. Research by Lee *et al.* [11] concluded that ES could promote the extension of nerve length by 40%–90%. Studies also reported that ES accelerated NGF-induced axon growth and synaptic signal transduction [12], so the application of ES did provide an effective way to promote central nervous regeneration.

Microfluidic chip technology has developed rapidly in the field of biomedicine with the advantages of high density, high throughput, high ease of integration, and portability [13–16]. When the poly(dimethylsiloxane) (PDMS) microfluidic device is applied to neurons cell culture platform, it can provide a microenvironment for physical and biochemical control through the guidance structure or microfluidic channel [17]. There were various multiple microfluidic chips used for neuron cell culture and study. Huang *et al.* [18] designed a micro-device for automatic cell culture, in which micro-pumps, micro-valves, and other micro-structures were designed to maintain the entry of cell culture fluid while expelling metabolic wastes, to realize automatic cell culture. Han *et al.* [19] constructed an *in vitro* three-dimensional model simulating the microenvironment *in vivo* based on PDMS microfluidic chip and conducted quantitative analysis on the differentiation of NSCs. The results showed that the fluid-controlled three-dimensional microenvironment greatly improved the differentiation ability of NSCs, compared with the traditional cell culture model. Shin *et al.* [20] also demonstrated that the microenvironment augmented the differentiation ability of NSCs.

At present, there have been some researches on the combination of microfluidics and microelectrodes. Konstantin *et al.* [21] focused on integrating the microfluidic devices with multi-electrode array (MEA) and the compatibility of reversible integration with MEAs and neuron networks *in vitro* was proved. In 2015, Lewandowska *et al.* [22] constructed a platform with microfluidics and MEA successfully achieved the separation of axons and somatic cells and recorded the electrophysiological signals of the cells in the channel. In 2017, Habibey *et al.* [23] bonded PDMS with low-density network microchannels and MEA to capture and amplify the weak extracellular activity from axons and realized the measurement of axon propagation speed.

In this paper, we developed a novel PDMS-based microfluidics device embedded with a microelectrode array which had both functions of stem cell culture and ES. A home-made signal generator was employed to output the bipolar symmetrical square wave onto rat NSCs as a model to observe the effect of ES on the growth, differentiation, proliferation, and other behaviors. We explored the effect of *in vitro* cell ES and then evaluated the positive significance of the microfluidic/micro-electrode composite micro-devices in the treatment of neurological diseases.

The designed microfluidic/microelectrode composite device was shown in Figs. 1a and b. The entire platform shape was designed as a 5 mm × 5 mm × 2 mm cuboid, consisting of a central microelectrode array and a surrounding microfluidic chip, as shown in Fig. 1c. The central microelectrode array was mainly used to complete the output of ES, and it was 4 mm × 4 mm distributed with tapered electrodes whose bottom diameter was 0.5 mm and height was 0.6 mm. The microscopic image of the tapered microelectrode was shown in Fig. 1d. While the microfluidic part achieved microfluidic control and cell culture, it was composed of one fluid inlet, one outlet, and two cell culture chambers, as shown in Fig. 1a. Between them were 0.2 mm wide microchannels. Cell injection, nutrient and metabolite entry and exit were accomplished through the inlet and outlet.

With the intrinsic advantages of high transparency and biocompatibility, PDMS was used as the substrate material of the microelectrode/microfluidic composite device. PDMS prepolymer and curing agent (Sylgard 184, Dow Corning, USA) were mixed at 10:1 (w/w) and poured onto the surface of the PMMA mold (Figs. S1 in Supporting information). After cured the device was pelt off and the microelectode array was obtained. The same method was used to obtain the microfluidic channel structure as seen in Fig. S1b1 and b2 (Supporting information). Then DC magnetron sputtering device (SBC-12, KYKY Technology Development Ltd., CN) was used to gold plating in the microelectrode surface as a conductive layer, wherein the coating thickness was 150 nm. Subsequently, the microelectrode was bonded with the microfluidic channel, and the conductive silver paste was used to connect the conductive layer and the wire. Finally, the multimeter (DT-9205, Hongda Instrument, CN) was used to confirm the conductive integrity of the microdevice and the impedance of each electrode was measured by a two-probe conductivity meter (2634B, Keithley, USA) through recording the current and the resistance over time in constant voltage mode. The impedance was about 14 Ω (Fig. S2 in Supporting information) and it can be found that the current changes slightly over time, thus proving the stability of the microelectrode array.

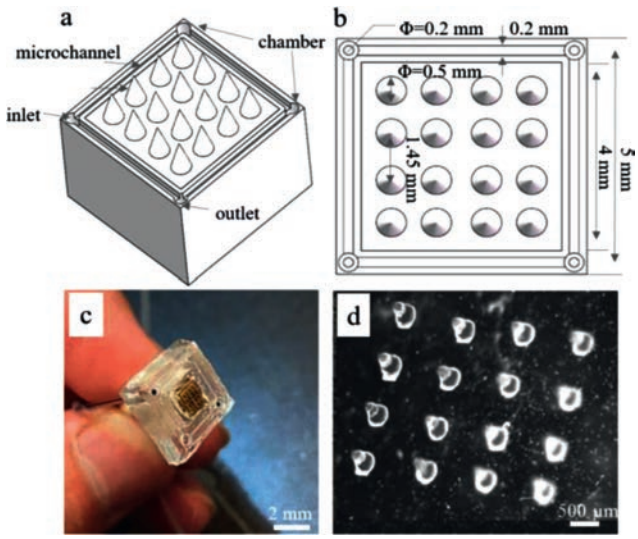

Fig. 1. Schematic of microfluidic/microelectrode composite microdevice: (a) 3D schematic of the microdevice. (b) Top view of the microdevice. (c) Physical picture of the microdevice. (d) Microscopic image of the tapered microelectrode.

The ES device was developed in our lab and the diagram was shown in Figs. 2a and b. It was connected to an oscilloscope to ensure electrical pulses delivered were mentioned as shown in Fig. 2c. The ES device was sterilized and kept for 30 min at 37 °C with a 5% CO_2 atmosphere before use. Biphasic current pulse ES has been widely used in nerve injury repair [24,25]. Therefore, the biphasic pulse was used, which can reduce not only the risk of irreversible Faraday reaction, but also the accumulation of charged protein around the electrode surface, and prevent the pH value increase during the stimulation [26–28]. Studies have shown that low-frequency and short-term electrical stimulation could promote the differentiation of stem cells, and then improve the regeneration ability of injured nerves [29–31]. Piacentini *et al.* [32,33] found that low-frequency electric field (50 Hz) can effectively enhance the differentiation of cortical NSCs into neurons *in vitro* and the neuronal differentiation rate of NSCs under electric field was higher than that of the non-electric field group through a series of studies. Therefore, in this experiment, the stimulation voltage was 1 V; pulse width was 200 μs and frequency was 50 Hz.

The cells used in the experiment were rat neural stem cells. The cells were recovered, inoculated and pass at the rate of 1:2–1:3 in a cell incubator at 37 °C with a 5% CO_2 atmosphere. After the cells state was stable, they were cultured in the cell culture dish and observed; then replaced with fresh complete medium every 2–3 days.

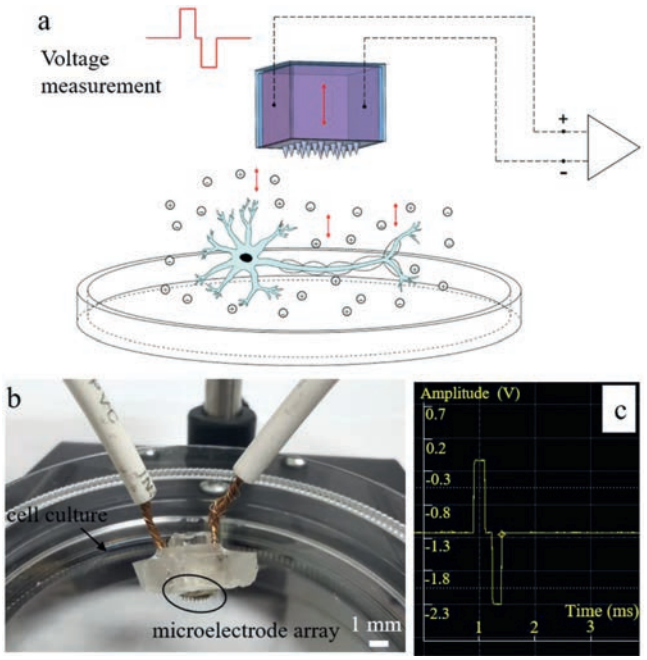

Fig. 2. (a) The microelectrode ES device diagram. (b) Setup image. (c) The oscillograph waveform.

After 5 days of incubation, the stimulation pulses were applied to the cells for 20 min per day and for 5 days continuously as the experimental group. During this period, the medium was replaced every next day. As a control, the cells were inoculated on the dish and cultured 5 days without electrical stimulation. The cells were observed and photographed under an inverted microscope at regular intervals every day. In the experiment, three parallel samples were used in each group, and the results were presented as mean ± standard deviation. The software of Sigmaplot 12.5 (Systat, CA, USA) was used for data analysis, independent sample t test and inter-group statistics, where $P < 0.05$ was defined significant.

The morphology of NSCs was first to observe the state of the cell spheres under an inverted phase-contrast microscope. The suspended cell spheres used in the experiment need to be relatively uniform in size, less adherent, small in the center black area, or no black area. The cell behavior was detected by immunocytofluorescence chemistry technique, in which the cell differentiation was detected by Nestatin and cell proliferation was detected by Brdu ELISA kit. As an intermediate filament type protein Nestin can be specifically expressed on neuroepithelial stem cells and is only expressed at the early stage of embryonic development in the neural epithelial, so as the neuron-specific markers. Therefore, Nestin was selected as the marker protein of rat NSCs, and the NSCs were co-stained with Nestin and DAPI by immunofluorescence. The ImageJ (NIH, USA) software was used to quantify the fluorescence intensity of Nestin, and the specificity rate of NSCs was obtained by calculating the ratio of the number of Nestin positive cells to the number of DAPI. Brdu is a derivative of thymine. It is often used to label newly synthesized DNA in living cells, which will be copied into daughter cells as the DNA is replicated [32,34]. The NSCs were co-stained with Brdu and DAPI by immunofluorescence, and the proliferation ability of NSCs before and after ES was observed. The fluorescence area of nerve cells was analyzed by the software ImageJ and obtained the cell proliferation rate.

The cell morphology without ES was observed as shown in Fig. 3a. After three days of culture, it was observed that the cells gathered around continuously, and several multicellular aggregates of different sizes appeared; on the 4th day, the number of single cells suspended in the culture flask decreased significantly, and the cells aggregated into compact sphere, namely neurosphere, with a diameter of 50–60 μm; on the 5th day, the sphere grew up to 80–90 μm in diameter, and it was regular, with good light permeability and no dark areas, indicating that the cells were in good condition. Therefore, the neurospheres cultured on the 5th day were selected for immunofluorescence staining identification.

Figures in the lower line of Fig. 3a demonstrated that ES significantly enhanced the cell growth compared to no treatment. On the third day of ES, the neurosphere became significantly larger. Therefore, ES can promote the proliferation of nerve cells within a certain time. On the 4th day of ES, dark areas were observed in the neurosphere indicating that the cells began to apoptosis. By the 5th day, it was found that the dark area changed to black, and the cells had died in large numbers. Fig. 3b showed the change of neurosphere diameter with the ES time. The neurosphere diameter was the largest on the third day of ES, and the diameter became significantly smaller when the stimulation continued. In addition, there was a significant difference ($P < 0.05$) in the neurosphere diameter after 2–4 days of stimulation compared with that without ES, it showed the cell diameter at the 3rd day of ES was approximately 1.56 times that of without stimulation. Therefore, it can be found that ES was beneficial to the growth and proliferation of nerve cells within a certain period, but when it exceeded a certain range, cells began to apoptosis. ES affected the molecules, ions, and regulatory factors of nerve tissue by changing the extracellular electric potential near the stimulated area. Therefore, when the stimulation time was too long, the extracellular electric potential was too high, and the calcium ions needed for cell growth could not be supplied and eventually lead to apoptosis.

Fig. 4a showed Nestin positive cells (green) and DAPI staining pictures (blue) as well as the image (Merge) obtained by merging the first two images. The whole-cell sphere without ES showed Nestin positive, indicating that the cells obtained after culture and passage were rat NSCs, which could be used for subsequent experimental studies on the behavior of NSCs. To further determine the cell Nestin positive rate, the spheres on the 5th day were digested into single-cell suspension, planted on the surface of the glass slide, and subjected to Nestin staining, observed, and counted under a fluorescence microscope, the result showed 98.3% ± 0.2% of the cells were Nestin positive, indicating that the subculture cells had the characteristics of NSCs and have high purity.

It could be seen from Fig. 4a that after ES three days, the volume of neurospheres has become significantly larger, which was consistent with the results observed in bright fields. Fig. 4b showed the statistical results of the Nestin positive rate before and after ES. After ES, 98.9% ± 0.4% of the cells were Nestin positive, indicating there was no significant difference between the two groups. Therefore, it can be concluded that NSCs can maintain good stem cell specificity while facilitating their proliferation after ES.

The neurospheres cultured 5th day without ES (as a control) and with 2–4 days ES were fixed and observed using an immunofluorescence microscope. The samples were stained with the rat Brdu antibody and DAPI. In Fig. 5a, followed by Brdu positive cells (red), DAPI staining (blue) images, and the former two images merged. As shown in Fig. 5a, the neurosphere volume after ES was significantly larger compared to the control, showing better proliferation. The cell proliferation rate after 2, 3 and 4 days of ES was calculated, respectively in Fig. 5b. When cells were subjected to a local electric field, they produced electrobiological behavior. After 2 days ES, cell viability was significantly increased, and the cell proliferation was 37.46% compared with that before ES. With the increase of the ES period, the relative proliferation reached 49.41% on the third day. During the first 3 days of electrical stimulation, the cell proliferation rate increased significantly (*P*

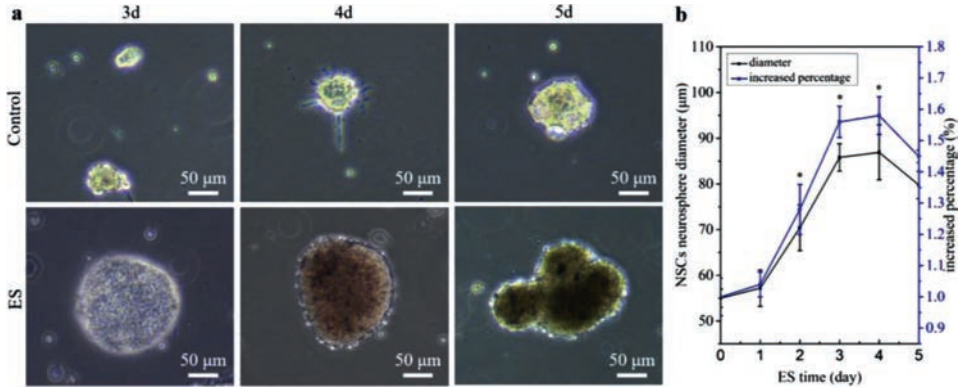

Fig. 3. (a) Culture morphology of NSCs neurosphere with and without ES. (b) Graph of neurosphere diameter with ES time ($^*P < 0.05$).

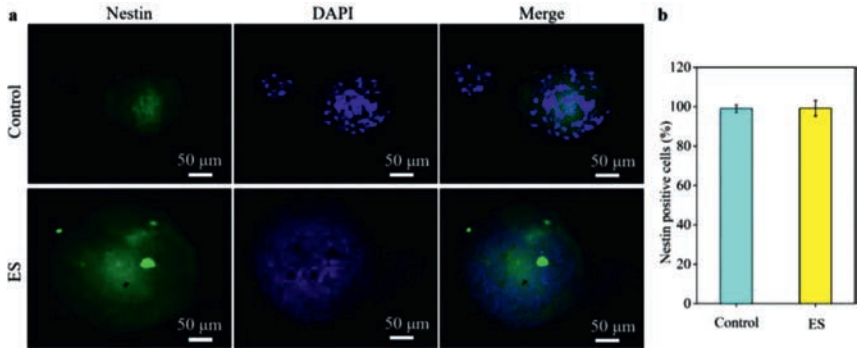

Fig. 4. (a) Immunofluorescence staining of NSC neurospheres with and without ES: Nestin-green, DAPI-blue. (b) The fluorescence quantitative results of Nestin expression.

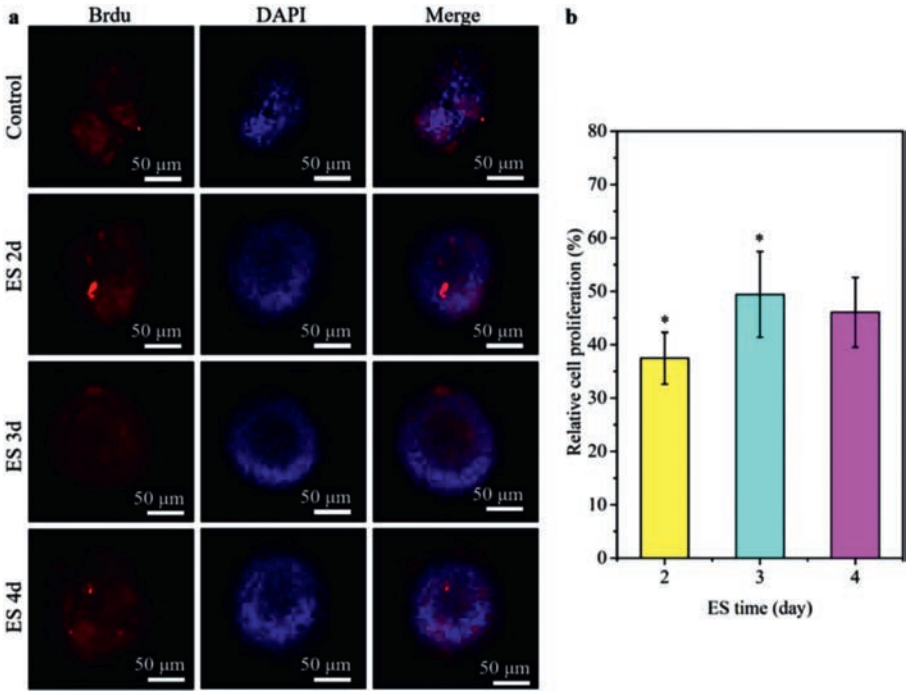

Fig. 5. (a) Immunofluorescence staining of NSCs neurospheres with ES at different days: Brdu-red, DAPI-blue. (b) The relative cell proliferation ($^*P < 0.05$).

< 0.05) compared with the control group. However, after 4 days of ES, it was observed that the neurosphere volume did not increase, and the proliferation rate was 46.06%, which was consistent with the growth state of cells observed in bright fields. A dark area appeared at the center of the neurosphere, indicating that the cells were beginning to apoptosis and the mortality was 1.21%. Therefore, it can be obtained that ES can promote the proliferation of NSCs to a certain extent.

In summary, we proposed a microfluidic and microelectrode composite microdevice that was simultaneous with electrical stimulation and cell culture function. The stimulated microelectrode array was designed and fabricated so that the electrode size and

spacing can more fully and evenly contact with cells to regulate cell behavior. This article preliminarily investigated the effect of ES on the behavior of NSCs *in vitro*, and the results indicated that ES had no significant effect on the specificity of NSCs, and extent promoted the differentiation of NSCs to some extent. Within a certain period, the appropriate ES can make the electronegative nerve cells generate a weak local electric field, and then increase the internal electric field to facilitate cell growth and proliferation. Therefore, the combinatorial treatment strategy may have a better therapeutic potential since ES may be used to promote the regeneration of NSCs, which is of reference significance for the repair of neural networks and the treatment of nervous system diseases.

Declaration of competing interest

The authors declare that they have no known competing financial interests or personal relationships that could have appeared to influence the work reported in this paper.

Acknowledgment

This work was financially supported by the Key Scientific and Technological Projects of the Beijing Education Commission (No. KZ201910005009).

Supplementary materials

Supplementary material associated with this article can be found, in the online version, at doi:10.1016/j.cclet.2021.08.006.

References

[1] N.V. Klinger, S. Mittal, Clin. Neurol. Neurosurg. 140 (2016) 11–25.
[2] S. Miocinovic, S. Somayajula, S. Chitnis, J.L. Vitek, JAMA Neurol. 70 (2013) 163–171.
[3] K. Seppi, D. Weintraub, M. Coelho, et al., Mov. Disord. 26 (2011) 42–80.
[4] X. Pu, X. Zhou, Z. Huang, G. Yin, X. Chen, Chin. Chem. Lett. 31 (2020) 1141–1146.
[5] D.H. Kim, J. Viventi, J.J. Amsden, et al., Nat. Mater. 9 (2010) 511–517.
[6] W. Jing, Q. Ao, L. Wang, et al., Chem. Eng. J. 345 (2018) 566–577.
[7] D. Xu, L. Fan, L. Gao, et al., ACS Appl. Mater. Interfaces 8 (2016) 17090–17097.
[8] A.K. Dubey, S.D. Gupta, B. Basu, J. Biomed. Mater. Res. Part B 98 (2011) 18–29.
[9] W. Zhu, T. Ye, S.J. Lee, et al., Nanomedicine 14 (2018) 2485–2494.
[10] L. Xiao, K.J. Gilmore, S.E. Moulton, G.G. Wallace, J. Neural Eng. 55 (2009) 260–271.
[11] J.Y. Lee, C.A. Bashur, A.S. Goldstein, C.E. Schmidt, Biomaterials 30 (2009) 4325–4335.
[12] Y.J. Chang, C.M. Hsu, C.H. Lin, S.C. Lu, L. Chen, Biochim. Biophys. Acta Gen. Subj. 1830 (2013) 4130–4136.
[13] M. Lei, Y. Zhang, Y. Li, Y. Lei, et al., Med. J. Wuhan Univ. 39 (2018) 610–614.
[14] A. Gokaltun, M.L. Yarmush, A. Asatekin, O.B. Usta, Technology 5 (2017) 1–12.
[15] T. Yuan, D. Gao, S. Li, Y. Jiang, Chin. Chem. Lett. 30 (2019) 331–336.
[16] Y. Zheng, Z. Wu, J.M. Lin, L. Lin, Chin. Chem. Lett. 31 (2020) 451–454.
[17] J. Park, H. Koito, J. Li, A. Han, Biomed. Microdevices 11 (2009) 1145–1153.
[18] C.W. Huang, S.B. Huang, G.B. Lee, J. Micromech. Microeng. 17 (2007) 783–786.
[19] S. Han, K. Yang, Y. Shin, et al., Lab Chip 12 (2012) 2305–2308.
[20] Y. Shin, K. Yang, S. Han, et al., Adv. Healthc. Mater. 3 (2013) 1457–1464.
[21] G. Konstantin, H. Grégoire, J. Nathan, et al., BioNanoSci 4 (2014) 263–275.
[22] M.K. Lewandowska, D.J. Bakkum, S.B. Rompani, A. Hierlemann, PLoS One 10 (2015) e0118514.
[23] R. Habibey, S. Latifi, H. Mousavi, et al., Sci. Rep. 7 (2017) 8558–8572.
[24] X. Luo, C.L. Weaver, D.D. Zhou, R. Greenberg, X.T. Cui, Biomaterials 32 (2011) 5551–5557.
[25] J.H. Lim, S.D. McCullen, J.A. Piedrahita, E.G. Loboa, N.J. Olby, Cell. Reprogramm. 15 (2013) 405–412.
[26] K. Wang, H.A. Fishman, H. Dai, J.S. Harris, Nano Lett. 6 (2006) 2043–2048.
[27] D.E. Moga, M.E. Calhoun, A. Chowdhury, et al., Neuroscience 125 (2004) 7–11.
[28] B. Ercan, T.J. Webster, Biomaterials 31 (2010) 3684–3693.
[29] A.N. Koppes, N.W. Zaccor, C.J. Rivet, et al., J. Neural Eng. 11 (2014) 2–13.
[30] T. Gordon, T.M. Brushart, N. Amirjani, K.M. Chan, Acta Neurochir. Suppl. 100 (2007) 3–11.
[31] J. Huang, Z. Ye, X. Hu, L. Lu, Z. Luo, Glia 58 (2010) 622–631.
[32] R. Piacentini, C. Ripoli, D. Mezzogori, G.B. Azzena, C. Grassi, J. Cell. Physiol. 215 (2008) 129–139.
[33] C. Grassi, M. D'Ascenzo, A. Torsello, et al., Cell Calcium 35 (2004) 307–315.
[34] C.A. Ariza, A.T. Fleury, C.J. Tormos, et al., Stem Cell Rev. Rep. 6 (2010) 585–600.